

Position Level Kinematics of the Atlas Motion Platform

R. Beranek and M.J.D. Hayes

*Carleton University, Department of Mechanical and Aerospace Engineering,
e-mail: jhayes@mae.carleton.ca; rberanek@connect.carleton.ca*

Abstract. Atlas is a novel six degree of freedom vehicle simulator motion platform where orienting is decoupled from positioning, and unbounded rotation is possible about any axis. Angular displacements are achieved by manipulating the spherical exterior of the cockpit with three omnivheel actuators. A significant challenge to practical implementation of the design is dynamic slip at each omnivheel-sphere interface. The dynamic slip renders the velocity level constraints non-holonomic, in turn meaning that the position level kinematics are undefined. This paper proposes a numerical integration algorithm to provide an estimate of the platform orientation. The algorithm is based on solving the associated quaternionic differential equation given constant omnivheel angular rates. For sufficiently small time intervals of changing omnivheel rates, the algorithm can be applied recursively to estimate the sphere position level kinematics given omnivheel angular velocity as input. Experimental results suggest that dynamic slip may be identified and compensated.

Key words: Unbounded angular displacement; position and velocity level kinematics; quaternionic differential equation; nonholonomic constraints.

1 Introduction

The Atlas motion platform [1] was introduced as a practical alternative to the Stewart-Gough hexapod [2, 3], used principally for motion simulator platforms. A table top technology proof-of-concept demonstrator is illustrated in Figure 1. The Atlas concept consists of a cockpit encased in a sphere which rests on three omnidirectional wheels. The three omnidirectional wheels are arranged on the edges of an equilateral triangle giving an angular separation of 120° in the XY -plane, see Figure 2(b). The elevation angle of each omnidirectional wheel relative to the XY -plane is 40° . The reason for the equilateral configuration is to achieve even force and torque distribution on the omnidirectional wheels, however the elevation angle of 40° was selected for ease of manufacturing and assembly. The sphere/omnivheel assembly is connected to three independent linear motion stages. The omnivheels control the orientation of the sphere, while the linear stages provide for the translation of the platform along all three linear axes. This allows for a full six degree of freedom (DOF) motion with unbounded rotation about any axis.

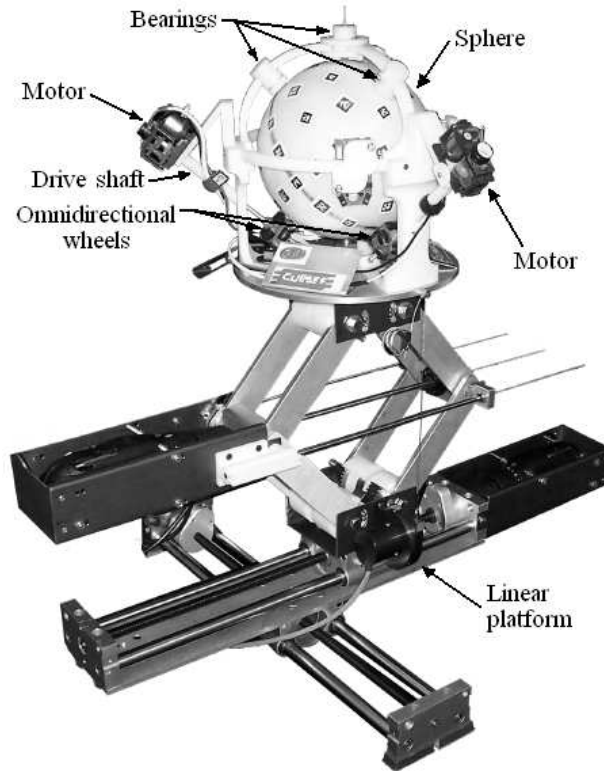


Fig. 1 The Atlas table-top 6-DOF demonstrator highlighting the omnidirectional wheel actuation concept.

The Atlas motion platform is not unique in its ability to provide unbounded angular displacement. For example, the Eclipse II architecture [4] possesses this ability. However, uniqueness of the Atlas platform lies in its kinematic model, which leads to remarkably simple, closed form velocity closure equations. Moreover, its orientation workspace is not constrained by structural interferences, or rotation limits of the spherical joints, compared to the Eclipse II.

One of the principal challenges for the Atlas concept is that the kinematics have so far only been defined at the velocity level [5]. The position level kinematics are undefined because the velocity constraints are nonholonomic due to the presence of dynamic slip at the omniwheel-sphere interface [6]. This paper presents an approach to estimate the Atlas platform orientation, starting from the velocity level kinematics derived in [5]. The approach consists of integrating the quaternionic differential equation [7, 8] assuming constant omniwheel angular velocity inputs. Measurements obtained from experiments yield information on how well the the quaternion solution estimates the orientation of the sphere for constant omniwheel

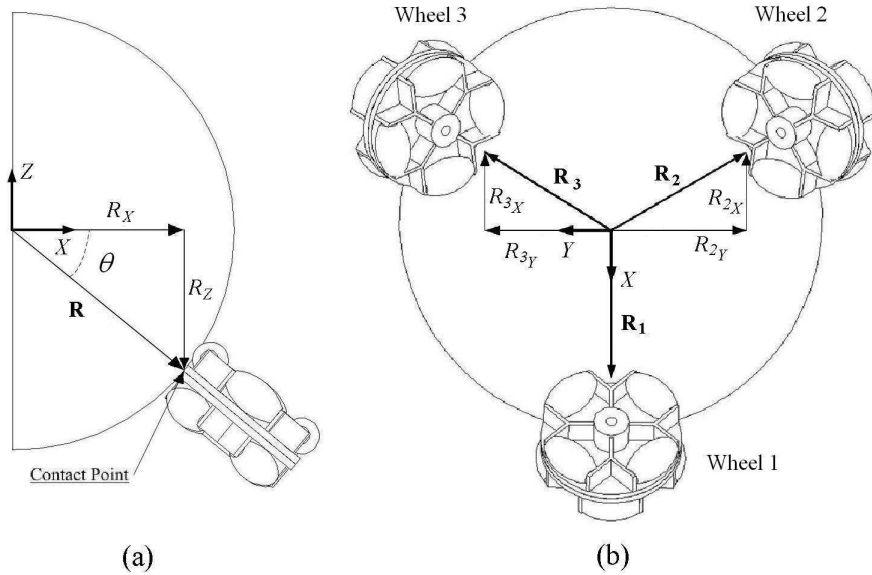


Fig. 2 Configuration of the original Atlas spherical platform: (a) front view; (b) bottom view.

speeds. A simple recursive algorithm for estimating orientation given nonconstant velocity inputs is also put forward.

2 Atlas Velocity Level Kinematic Model

The velocity level kinematic model of the Atlas platform is derived in detail in [5], and is briefly summarized in what follows. The translational displacements generated with the XYZ linear platform are completely decoupled from the rotational displacements of the sphere. Modelling the linear velocity of the geometric centre of the sphere is straightforward and typically represented as a simple linear term which must be added to the more demanding spherical kinematic model. Therefore, without loss in generality, only the spherical kinematics need be considered here.

It is convenient to perform velocity analysis of a manipulator with its Jacobian. It is, by definition, a mapping between time rates of change. By convention, in robotics it is the mapping between the time rates of change of the joint variables to the time rates of change of the position and orientation of the end effector [9].

Changes in orientation of the Atlas motion platform are achieved with three active omnidirectional wheels arranged on the edges of an equilateral triangle giving an angular separation of 120° in the XY -plane, see Figure 2(b). The elevation angle of each omnidirectional wheel relative to the XY -plane is $\theta = 40^\circ$. The radius of the

table top demonstrator sphere is $R = 10.16$ cm, while the radius of each omnivheel is $r = 2.00$ cm.

For this configuration of omnidirectional wheels the resulting mapping between the velocities in *joint space* and those in *Cartesian space* is:

$$\Omega = \mathbf{J}\omega = \frac{r}{3R} \begin{bmatrix} -2 \csc \theta & \csc \theta & \csc \theta \\ 0 & \sqrt{3} \csc \theta & -\sqrt{3} \csc \theta \\ -\sec \theta & -\sec \theta & -\sec \theta \end{bmatrix} \begin{bmatrix} \omega_1 \\ \omega_2 \\ \omega_3 \end{bmatrix}, \quad (1)$$

where Ω is the angular velocity vector of the sphere expressed in the inertial sphere coordinate system illustrated in Figure 2, \mathbf{J} is the Jacobian of the manipulator, and ω is the array of angular rates of the three actuating omnivheels, r represents the radius of the omnivheel (assuming all three to be equal), R is the external radius of the sphere, and θ is the elevation angle of each omnivheel. Substituting the numerical values for r , R , and θ leads to

$$\mathbf{J} = \begin{bmatrix} -0.2042 & 0.1021 & 0.1021 \\ 0 & 0.1768 & -0.1768 \\ -0.0856 & -0.0856 & -0.0856 \end{bmatrix}. \quad (2)$$

Inspection of the system Jacobian expressed by either Equation (1) or Equation (2) reveals that, unlike typical manipulator Jacobians, \mathbf{J} is time invariant and depends only on design constants. These constants can be chosen such that the Jacobian will possess full rank and that the orienting workspace of the sphere is configurationally singularity free. Moreover, because the sphere can have any orientation about any point within reach of the sphere centre, the reachable workspace is fully dexterous.

Because the Jacobian of the system is time invariant and constant, once the configuration has been determined, acceleration-level kinematics can be obtained by simple differentiation of the expression, yielding:

$$\dot{\Omega} = \mathbf{J}\dot{\omega}. \quad (3)$$

3 Atlas Position Level Kinematic Model

Obtaining the expression for the orientation of the platform, however, is not as simple. In this work quaternions are employed because the unbounded and singularity-free nature of the design calls for a singularity-free representation. Integration of the quaternionic differential equation is required [8]:

$$\dot{q} = \frac{1}{2} \Omega \circ q, \quad (4)$$

where q is the unit quaternion describing the orientation of the system, and $\Omega \circ q$ is a quaternion product.

The quaternion product can be expressed as a matrix product [7]:

$$\frac{d\mathbf{q}}{dt} = \mathbf{F}_q(\boldsymbol{\Omega})\mathbf{q}, \quad (5)$$

where $\mathbf{F}_q(\boldsymbol{\Omega})$ is a skew symmetric matrix of the sphere angular velocities expressed in the sphere inertial coordinate system, and is defined to be:

$$\mathbf{F}_q(\boldsymbol{\Omega}) = \frac{1}{2} \begin{bmatrix} 0 & -\Omega_x & -\Omega_y & -\Omega_z \\ \Omega_x & 0 & \Omega_z & -\Omega_y \\ \Omega_y & -\Omega_z & 0 & \Omega_x \\ -\Omega_z & -\Omega_y & -\Omega_x & 0 \end{bmatrix}. \quad (6)$$

Equation (5) yields a set of four simple ordinary differential equations. If the angular velocity $\boldsymbol{\Omega}$ is constant and the initial conditions $\mathbf{q}(t_0)$ are known, then the solution to Equation (6) can be written as [10]

$$\mathbf{q}(t) = \phi_q(t_0, t, \boldsymbol{\Omega})\mathbf{q}(t_0), \quad (7)$$

such that the transition matrix is

$$\phi_q(t_0, t, \boldsymbol{\Omega}) = e^{\mathbf{F}_q(\boldsymbol{\Omega})\Delta t} = \cos(\|\boldsymbol{\Omega}\|\Delta t/2)\mathbf{I} + 2\frac{\sin(\|\boldsymbol{\Omega}\|\Delta t/2)}{\|\boldsymbol{\Omega}\|}\mathbf{F}_q(\boldsymbol{\Omega}), \quad (8)$$

with $\Delta t = t - t_0$, and $\|\boldsymbol{\Omega}\| = \sqrt{\Omega_x^2 + \Omega_y^2 + \Omega_z^2}$.

The solution represented by Equation (7) can be expressed as the quaternion product

$$\mathbf{q}(t) = \mathbf{q}(t_0) \circ \phi_q(t_0, t, \boldsymbol{\Omega}), \quad (9)$$

or

$$\mathbf{q}(t) = \begin{bmatrix} q(t_0)_1 & -q(t_0)_2 & -q(t_0)_3 & -q(t_0)_4 \\ q(t_0)_2 & q(t_0)_1 & -q(t_0)_4 & q(t_0)_3 \\ q(t_0)_3 & q(t_0)_4 & q(t_0)_1 & -q(t_0)_2 \\ q(t_0)_4 & -q(t_0)_3 & q(t_0)_2 & q(t_0)_1 \end{bmatrix} \begin{bmatrix} \cos \frac{\|\boldsymbol{\Omega}\|t}{2} \\ \frac{\Omega_x}{\|\boldsymbol{\Omega}\|} \sin \frac{\|\boldsymbol{\Omega}\|t}{2} \\ \frac{\Omega_y}{\|\boldsymbol{\Omega}\|} \sin \frac{\|\boldsymbol{\Omega}\|t}{2} \\ \frac{\Omega_z}{\|\boldsymbol{\Omega}\|} \sin \frac{\|\boldsymbol{\Omega}\|t}{2} \end{bmatrix}. \quad (10)$$

Given the magnitudes of the three omnivheel angular rates, the corresponding angular velocity of the sphere is determined using Equation (1). The subsequent orientation of the sphere at any time t after an initial time t_0 is then estimated using Equation (10), ignoring the effects of dynamic slip.

4 Experimental Validation

To validate the solution provided by integrating the quaternionic differential equation, several simple cases were examined where omnivheel constant angular rates were specified and the corresponding sphere angular velocity was measured. For the first three, each angular velocity was selected such that it caused the sphere to spin about one of its inertial axes according to Equation (1). The resulting motion of the table top demonstrator (Figure 1) observed appeared to be consistent with the model.

To validate Equation (10) an arbitrary axis for the rotation of the sphere was selected using arbitrary constant angular velocities for each omnivheel. The sphere motion predicted by Equation (10) was compared to motion data recorded. The measurement system consists of a three axis gyroscope (MicroStrain 3DM-GX1) mounted inside the sphere and a camera-based external motion system that tracks the relative displacement of markers on the surface of the sphere, see Figure 3. Ideally, the nondeterministic gyroscope drift is zeroed with data from the external camera-based system and the internal sensor data are fused using unscented Kalman filter techniques [11]. However, the vision system is not functioning reliably yet and only gyroscope data is currently available.

Several experiments were run where omnivheel angular rates were specified and the resulting motion of the sphere was tracked and recorded as output from the three axis gyroscope. The time history of the angular displacements about the sphere inertial axes that was predicted is in the same ball park as those measured for all runs. Results, comparing predicted and measured orientation about the inertial coordinate system, from a run where the three omnivheel angular velocities were prescribed as $[\omega_1, \omega_2, \omega_3] = [5, -5, 5]$ rads/s are illustrated in Figure 4. The relatively large tracking drift in yaw, pitch, and roll is likely due to the nondeterministic drift of the gyroscopes. However, it may also be partly due to random errors associated with dy-

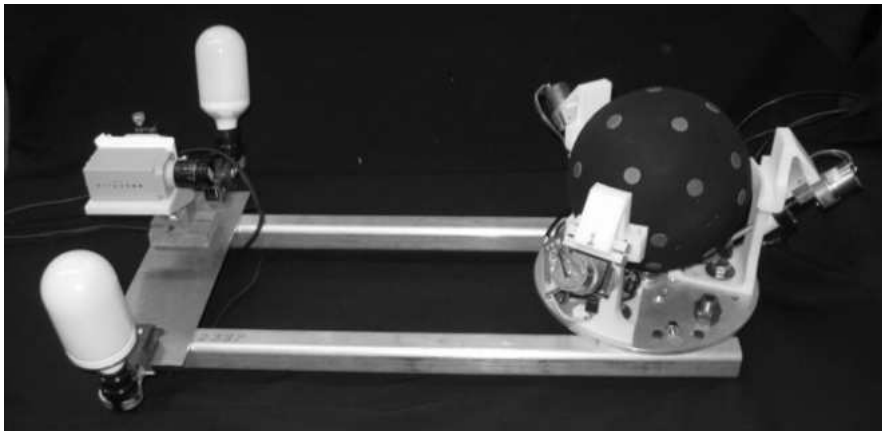


Fig. 3 Sphere orientation measurement system.

dynamic slip and variation in omniwheel angular velocities. Nevertheless, the results suggests that position level kinematics modelled by Equation (10) are representative of the physical system if the dynamic slip is identified with the measurement system and compensated.

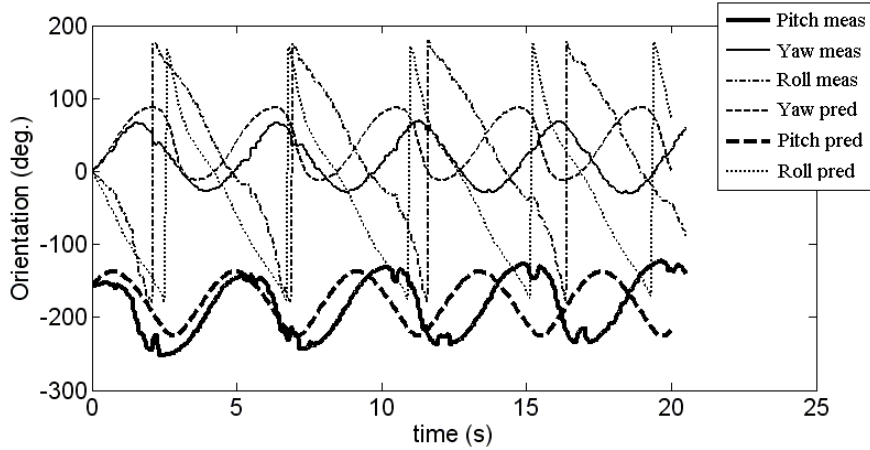


Fig. 4 Predicted and measured sphere angular velocities.

5 Orientation Estimate For Nonconstant Velocity Inputs

The solution determined with the integration of the quaternionic differential equation is only valid for constant omniwheel angular velocities. Regardless, this solution can be used in a numerical integration algorithm to provide an estimate of the sphere orientation for a general trajectory. The relation expressed by Equation (9) can be used to construct a recursive estimate. Consider

$$\mathbf{q}(k) = \mathbf{q}(k-1) \circ \phi_q(\Delta t, \boldsymbol{\omega}(k-1)), \quad (11)$$

where k is a time index and Δt is the time interval between omniwheel velocity measurements.

The solution is therefore a recursive estimate where the orientation is an extrapolation given the previous angular velocities of the omniwheels and previous orientation at time $k-1$. For sufficiently small Δt , the assumption that the motion between time steps is linear may be used and a reasonable estimate of the sphere orientation can be obtained for any general set of omniwheel angular velocities over an arbitrary trajectory.

6 Conclusions

Because of the presence of dynamic slip at each sphere-omniwheel interface, the velocity level kinematic constraints of the Atlas sphere are nonholonomic. The orientation of the sphere at any time t given constant omniwheel angular velocity inputs can be predicted using the solution to a quaternion based differential equation. The predicted time history of the change in orientation of the sphere possesses the same tendencies as the measured change in orientation, however measured values tend to drift, and there appears to be some bias about some inertial coordinate system axes. The drift may give an indication of error imposed by the dynamic slip, and could possibly be used for error correction, however the gyroscope drift must first be zeroed.

This solution can also be adapted to a numerical integration algorithm which can effectively be used as a general solution to the platform kinematics, providing an estimate of the platform orientation for any set of varying omniwheel input. This may allow for a good estimate of the orientation that could, in combination with the measurement system, be used in the control algorithm for the platform. Future work will focus on experimental validation of the constant angular velocity solution as well as validation of the proposed numerical solution.

References

1. M.J.D. Hayes, R.G. Langlois: "Atlas: A Novel Kinematic Architecture for Six DOF Motion Platforms". In: *Transactions of the Canadian Society for Mechanical Engineering*, vol 29, no 4, pp. 701-709 (2005)
2. V.E. Gough: "Contribution to Discussion of Papers on Research in Automobile Stability, Control and Tyre Performance". In: *Proc of Auto Div. Inst. Mech. Eng.*, pp. 392-394 (1956)
3. D. Stewart: "A Platform with 6 Degrees of Freedom". In: *Proc. of the Institution of Mechanical Engineers*, vol. 180, Part 1, no. 15, pp. 371-378 (1965)
4. J. Kim, J.C. Hwang, J.S. Jim, C.C. Iurascu, F.C. Park, Y.M. Cho: "Eclipse II: A New Parallel Mechanism Enabling Continuous 360-Degree Spinning Plus Three-Axis Translational Motions". In: *IEEE Transactions on Robotics and Automation*, vol. 18, no. 3, pp. 367-373 (2002)
5. M.J.D. Hayes, R.G. Langlois, A. Weiss: "Atlas Motion Platform Generalized Kinematic Model". In: *Proceedings of the Second International Workshop on Fundamental Issues and Future Research Directions for Parallel Mechanisms and Manipulators*, Montpellier, France, pp. 227-234 (2008)
6. J.H. Ginsberg: "Advanced Engineering Dynamics", 2nd edition. Cambridge University Press (1995)
7. S. Särkkä: "Notes on Quaternions". Internal Technical Document, Helsinki University of Technology (2007). <http://www.lce.hut.fi/~ssarkka/>. Cited 15 Jan 2010
8. A.L. Schwab, J.P. Meijaard: "How to Draw Euler Angles and Utilize Euler Parameters" In: *Proceedings of ASME IDETC/CIE* (2006)
9. J.C. Craig: "Introduction to Robotics", 2nd edition. Addison Wesley (1989)
10. D. Zwillinger. "Handbook of Differential Equations", 3rd edition. Academic Press (1998)
11. J. Linseman. "A UKF-Based Orientation Estimator for the Atlas Platform". M.A.Sc. Thesis, Dep't. of Mech. & Aero. Eng., Carleton University, Ottawa, ON, Canada (2010)